Nuclear Inst. and Methods in Physics Research, A 1041 (2022) 167410

Contents lists available at ScienceDirect

Nuclear Inst. and Methods in Physics Research, A

journal homepage: www.elsevier.com/locate/nima

A large area efficient trigger scintillator with SiPM read out

D. Grzonka [a,*], P. Bergmann [a], T. Hahnraths von der Gracht [a], P. Kulessa [b], W. Parol [e], T. Sefzick [a], J. Ritman [b,c,a], M. Zielinski [d]

[a] Institut für Kernphysik, Forschungszentrum Jülich, 52428 Jülich, Germany
[b] GSI Helmholtzzentrum für Schwerionenforschung GmbH, 64291 Darmstadt, Germany
[c] Ruhr-Universität Bochum, Institut für Experimentalphysik I, 44801 Bochum, Germany
[d] M. Smoluchowski Institute of Physics, Jagiellonian University, 30-348 Kraków, Poland
[e] The Henryk Niewodniczański Institute of Nuclear Physics PAS, 31-342 Kraków, Poland

ARTICLE INFO

Keywords:
Scintillation detector
SiPM

ABSTRACT

A large area plastic scintillator detector system with SiPM read out has been prepared in order to improve the trigger selectivity for reaction studies induced by an intense proton beam with a beam momentum of several GeV/c. The system consists of six trapezoidal modules, each with three plastic scintillator elements that are each equipped with 12 SiPMs. The detection of a charged particle is based on registering coincident signals in several SiPMs. By requiring a signal on at least two of the SiPMs, the noise rate is negligible and a detection efficiency close to 100% is achieved.

1. Introduction

Plastic scintillators are widely used for charged particle detection in various fields. They can cover large areas in any customized geometry with thicknesses adapted to the tolerable energy loss. In typical applications plastic scintillators are read out by conventional photomultipliers using a light guide to collect the photons and transform the scintillator to the photomultiplier geometry. Such a solution has some drawbacks in terms of required space and tolerance to magnetic fields. With the advent of Silicon photomultipliers (SiPM) an alternative photon detector is available. SiPMs consist of an array of separate avalanche photon diodes operated in the Geiger-mode with quench resistors to stop the avalanche process, see [1,2] for detailed descriptions. SiPMs are used in a large number of applications in particles and nuclear physics [2] and also in other fields [3,4]. They allow a simplified detector construction especially in applications with severe geometrical restrictions which is the case for the requested additional detector component for HADES [5,6].

The HADES detector is an external magnetic spectrometer installed at GSI for hadronic interaction studies. It has a sixfold symmetric structure around the beam with six toroidal superconducting magnet coils and the volume between the coils is filled with various detector components. For precise proton induced hyperon and light meson production studies an improved trigger selectivity is highly desired [7]. Therefore a new scintillator detector called the Inner TOF (iTOF) has been prepared. The new detector consists of 6 modules surrounding the beam in a conical arrangement, as shown in Fig. 1. The available space is rather limited which requires a flat design with a thickness of about 1 cm including the signal read out. Furthermore only photon sensors insensitive to magnetic fields can be used. Therefore SiPMs were chosen for the read out of the scintillation light. SiPMs are quite small and can be directly coupled to a scintillator. Moreover they have a high photon detection efficiency and a high gain, operate with a low bias voltage and they are insensitive to magnetic fields. One drawback is the high dark count rate compared to a conventional photomultiplier. But with a selection of coincident signals in several SiPMs a real signal can be well separable from the dark current.

2. InnerTOF design

Each single iTOF-module has a trapezoidal shape with a height of about 740 mm and a width of about 700 mm at the long edge and about 90 mm at the short edge (as shown in Fig. 2). An iTOF-module includes three separate plastic scintillators, wrapped individually in several layers of aluminum foil (foil-thickness = 5 μm) and black PE-foil (foil-thickness = 10 μm) to ensure a light tight package. The scintillator material BC-408 from Saint-Gobain [8] with a nominal thickness of 6.4 mm is used, see Table 1 for some characteristics. The three scintillators are linked with thin tape and placed in an aluminum frame. The insensitive gap between the scintillators is less than 0.2 mm and the aluminum frame is only at the outer edge of the scintillator package. At the long edge of the frame there is a free space of about 1 cm width between the scintillator and aluminum frame for the installation of the SiPMs. Cross sectional views of the side and of the long edge with SiPMs are shown in Fig. 2.

* Corresponding author.
E-mail address: d.grzonka@fz-juelich.de (D. Grzonka).

https://doi.org/10.1016/j.nima.2022.167410
Received 8 July 2022; Received in revised form 18 August 2022; Accepted 24 August 2022
Available online 31 August 2022
0168-9002/

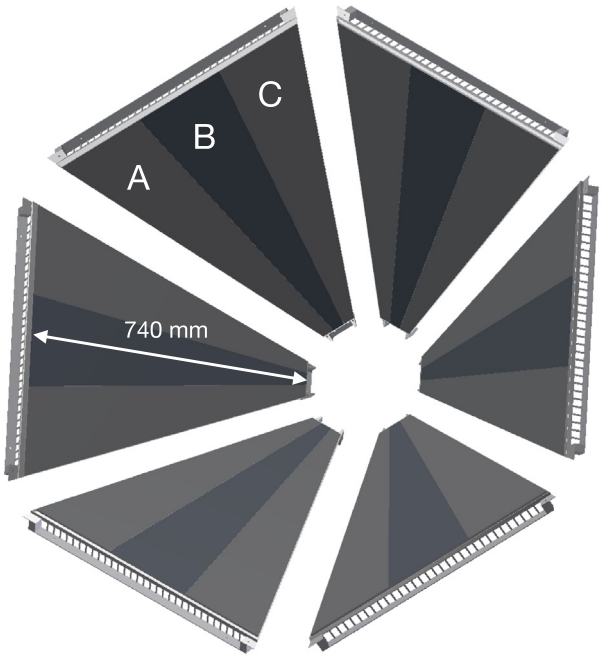

Fig. 1. Sketch of the iTOF detector system which consists of six modules each with three separate scintillators (A, B, C).

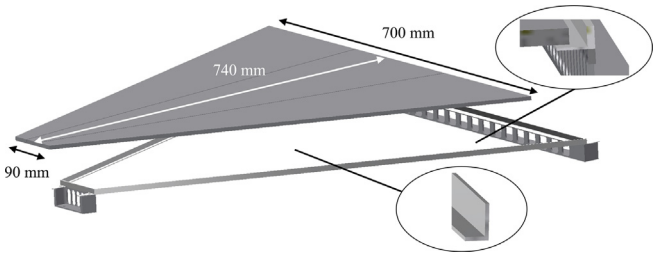

Fig. 2. Structure of an iTOF detector element including three separate scintillators in one common Al-frame. In the ellipses the cross sections of the side and the long edge are sketched.

3. Photon read out

Because of the space limitation in the HADES apparatus, the design of the photon readout had to be small and robust to enable easy mounting without interference with other detectors. Moreover the desired position of the new detector is influenced by a strong, inhomogeneous magnetic field, which makes it difficult to use standard vacuum photomultipliers. For that reason the scintillator light output is read out by silicon photomultipliers (SiPM). SiPMs of the type MicroFC-60035 from OnSemi [9] with an active area of 6 mm × 6 mm are used. Several important characteristic parameters of the SiPMs are listed in Table 1. A useful feature of the chosen SiPM-type is the availability of a fast output signal generated by an internal capacitor. For the final design four SiPMs were soldered to a printed circuit board. The SiPM-boards include only passive components for the signal read out, a temperature sensor (TMP37G) and sockets for FFC-cables. There is no amplification stage on the board and the signals are directly read out by the frontend electronics. Fig. 3 shows a photograph of the SiPM-board with four SiPMs on the front and the sockets with the temperature sensor on the back. The electronic circuit is shown on the right side of Fig. 3. Three of these SiPM-boards were attached to the long edges of each scintillator.

Before the SiPM-boards were attached to the iTOF-scintillators they were tested by mounting them on a small test scintillator irradiated

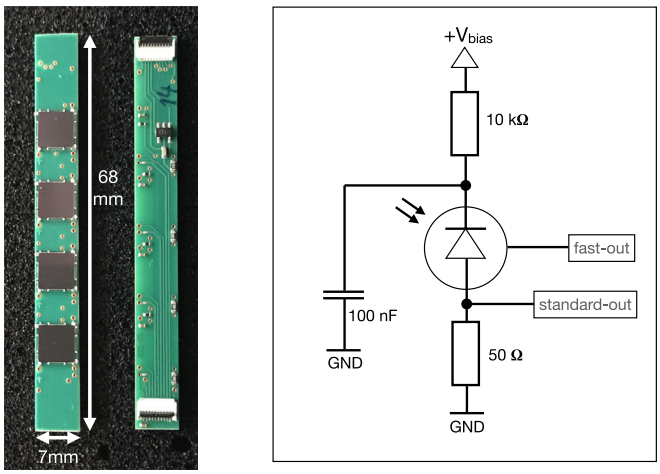

Fig. 3. SiPM-board with four SiPMs (MicroFC-60035) on the front and some passive components, temperature sensor and sockets on the back with the electronic circuit.

Table 1
Characteristics of BC-408 and MicroFC-60035.

Characteristics of the scintillator BC-408		
Light output (% Anthracene)	:	64%
Peak wavelength	:	425 nm
Bulk light attenuation length	:	380 cm
Pulse width (FWHM)	:	~2.5 ns
Characteristics of MicroFC-60035		
SiPM size	:	7×7 mm^2
Microcells and size	:	18980 cells, 35 μm
Fill factor	:	64%
Peak wavelength	:	420 nm
Breakdown voltage (V_{br})	:	~24.5 V
PDE at V_{br} + 5 V	:	41%
Rise time (fast out)	:	1.0 ns
Pulse width (FWHM, fast out)	:	3.2 ns

by a ^{90}Sr-source. An exemplary test result of a single SiPM-board is shown in Fig. 4 where the four fast and standard signals from individual SiPMs of the board are displayed at a four-channel scope operated in persistence mode. The typical signal height is 5 to 10 mV and the signal width is 15 to 20 ns (FWHM) for the fast signals and 200 to 300 ns for the standard signals. The scope was triggered by the yellow trace (marked in Fig. 4) and for all events we see always a signal for all four SiPMs, which indicates a high efficiency for the detection of the scintillation light. The coupling between scintillator and SiPM was done by 1 mm thick Silicon-pads. In Fig. 5 a single SiPM-board coupled to the scintillator and the whole scintillator edge with three SiPM-boards connected via FFC cables to an adapter board is shown. The adapter-board plays a role of an interconnection between the three SiPM boards and one PaDiWa board [10,11] used for the signal read out. PaDiWa is the acronym for PANDA-DIRC-WASA, detector systems for which the board was developed. The adapter-board is equipped with FFC sockets and two connectors, a supply connector (AMPMODU 280380-2) for the power supply lines for the three SiPM-boards, the power supply for the temperature sensor and the temperature output and a connector (TMMH-116-01-T-D-RA) for the PaDiWa-board. It connects the 12 separate fast signals of the SiPMs to the PaDiWa input and in addition from each SiPM-board the standard signals of the four SiPMs are summed and connected to the PaDiWa-input. The PaDiWa-board used here includes a 16-channel amplifier with an amplification of about a factor 10 and a discriminator to generate logic signals which are passed to a TRB3 board (General Purpose Trigger and Readout Board — generation 3) [10,12]. The signal processing and discrimination is implemented in a FPGA on the PaDiWa-board. LVDS signals (Low Voltage Differential Signaling) are generated for both, the leading and

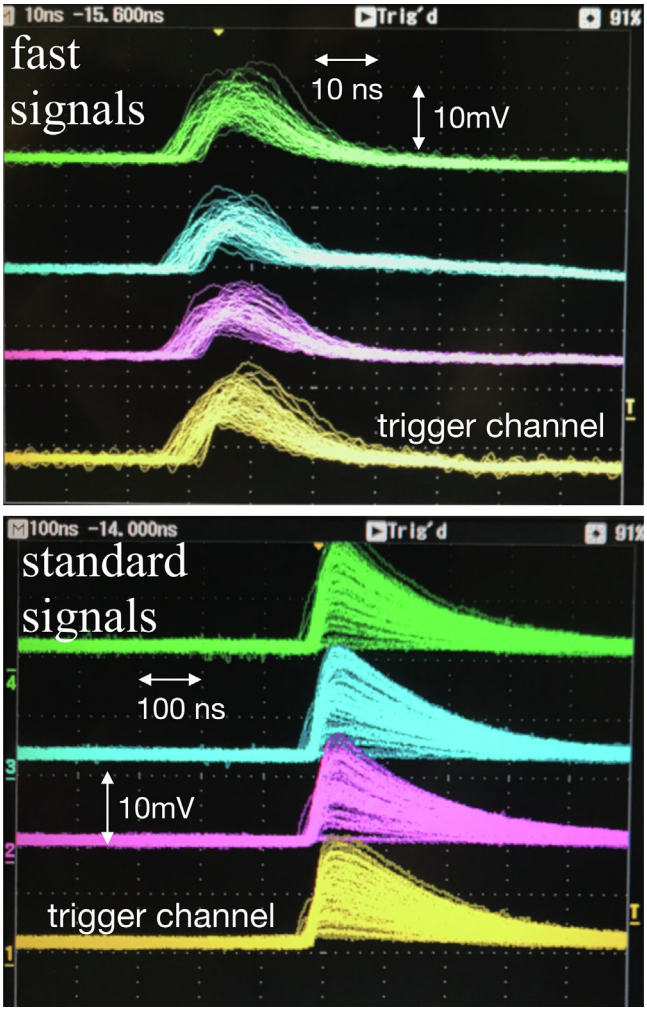

Fig. 4. Typical fast and standard signals of a SiPM-board when irradiated by a ^{90}Sr-source. The output signals of the SiPM-board are directly connected to a four-channel scope operated in persistence mode.

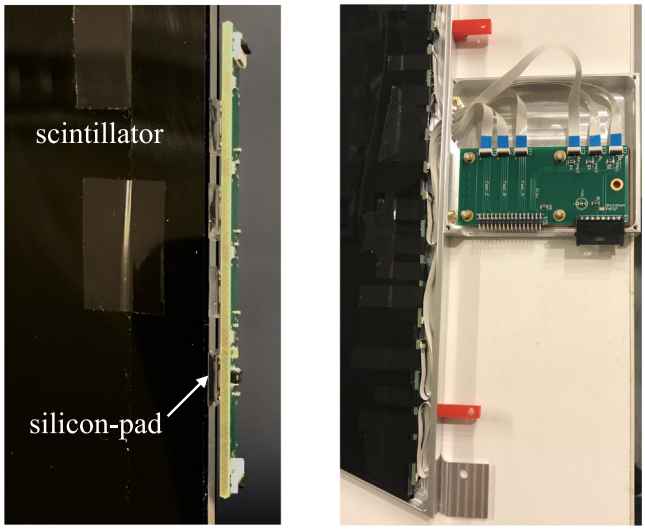

Fig. 5. SiPM-board attached to the scintillator edge coupled by silicon pads (left) and the final read out of one scintillator with FFC cables used to pass the SiPM-signals to an adapter-board (right).

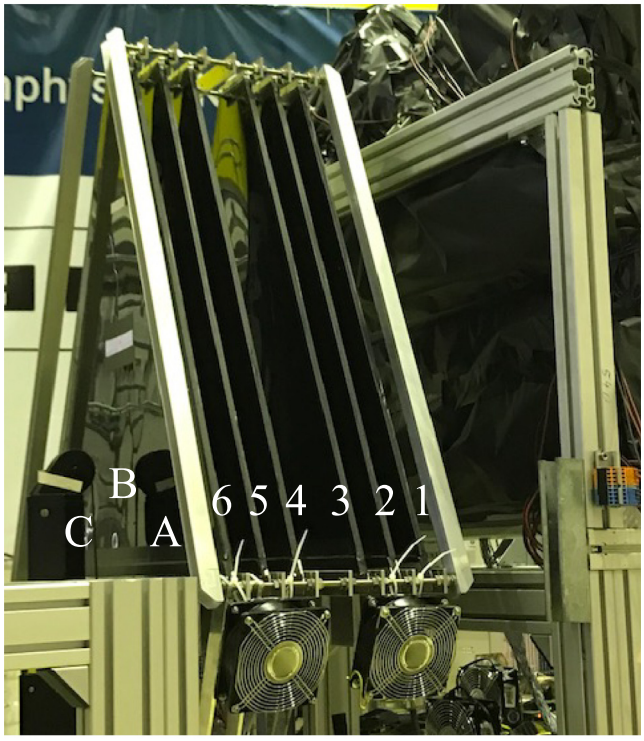

Fig. 6. Arrangement of the iTOF-modules for measurements with proton beam and cosmic particles. For the tests with cosmic particles the stack was rotated by 90°.

trailing edge of the SiPM signals to extract the amplitude information by the time-over-threshold method. The TRB3 board includes four FPGA based TDCs with a time precision below 20 ps and in total 264 channels. An additional central FPGA serves as flexible trigger system and manages slow control and read-out of the peripheral FPGAs over a gigabit Ethernet connection.

The individual fast signals and the sum signals were investigated with a ^{90}Sr source placed at various positions on the scintillators by connecting the signal lines at the adapter-board directly to a scope. The fast SiPM-signals were comparable to the distributions shown in Fig. 4 with amplitudes of 5 to 10 mV for all scintillator positions.

In independent studies [13], these SiPMs were confirmed to have sufficient radiation tolerance for the operation in the planned experiments.

4. Tests of the iTOF modules with proton beam and cosmic radiation

In addition to qualitative source tests, all iTOF-modules were tested with cosmic particles and with a proton beam at the COSY synchrotron in Jülich [14]. For the test with protons we used a beam momentum of 2.74 GeV/c which is close to minimum ionizing particles. All six iTOF-modules were mounted in a frame parallel to each other so that the beam passed though all modules. Fig. 6 shows the arrangement of the iTOF-modules for the measurements with the proton beam. In order to cover the whole scintillator area with the proton beam the iTOF-stack was moved to various positions. Two small plastic scintillators with an area of 8 cm × 8 cm were installed upstream and downstream of the iTOF-stack to generate a trigger signal for the data acquisition system. The calculated average energy loss in each iTOF scintillator assuming the nominal thickness of 6.4 mm and considering the energy reduction on the way to the iTOF-scintillators amounts to about 1.31 MeV for each scintillator in the stack compared to 1.295 MeV for minimum ionizing particles.

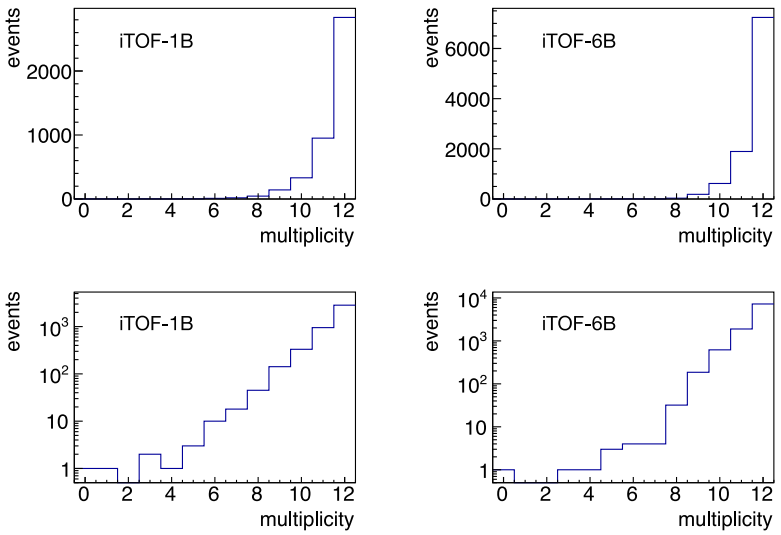

Fig. 7. Distribution of the fast SiPM signal multiplicity for the middle scintillators resulting from a proton beam position in the scintillator center. In the upper plot the distribution is shown in a linear scale and in the bottom part the same distributions are shown with a logarithmic scale. The difference in the event rates are due to different entries in multiplicity = 12 in the neighboring modules.

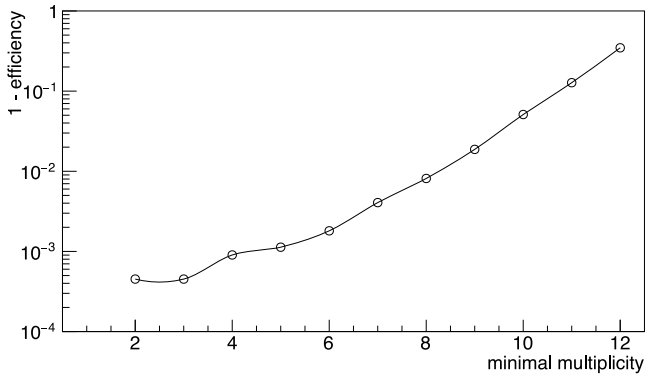

Fig. 8. Efficiency loss for the detection of a beam proton as a function of the minimum requested SiPM-signal multiplicity for iTOF-module no.1.

The measurements were performed in the same way as in the operation at the HADES detector. The SiPM signals were read out by PaDiWa-boards which were connected to a TRB3 based data acquisition system. The leading and trailing edges of all signals were registered, which allowed not only the start time to be determined, but also the signal amplitude to be reconstructed by evaluating the time over threshold measurement. The discriminator thresholds in the PaDiWa-board were set to an amplitude of about 2 mV and the multiplicity of fast SiPM-signals exceeding the threshold value was determined. Such a procedure will be used for the operation of the iTOF-detector in the HADES experiment. The signal rates of a single SiPM for this setting were in the range of 10 to 20 signals/s without beam and with beam the rate on a single SiPM was 10^4 to 10^5 signals/s, a rate which is also expected in the HADES experiment. The trigger rate for the data acquisition system was in the order of 10^3 trigger/s.

Fig. 7 shows the multiplicity distribution of the fast SiPM signals of the first (no.1) and last (no.6) iTOF-modules. As mentioned above, events were selected which have coincident signals in the small scintillators upstream and downstream of the stack of iTOF detectors. Furthermore to ensure that a beam particle passed through the iTOF-module under consideration, neighboring modules were required to have signal multiplicities equal to 12 (for iTOF-module no.1: $M_3 = 12$ and $M_4 = 12$ (the power supply for iTOF-module no.2 was switched off during this test), for iTOF-module no.6: $M_4 = 12$ and $M_5 = 12$). The data in Fig. 7 were taken for a centered stack position where the beam passed through the center of the middle scintillators. In more than 60% of the events all 12 SiPMs have a signal and for multiplicities M≥9 already 95% of the events are included. With a multiplicity threshold in the range of M> 4 efficiencies of about 100% were achieved. Fig. 8 shows the efficiency loss (1-efficiency) of iTOF-module no.1 as a function of the minimum required multiplicity.

Comparable multiplicity distributions were seen for other beam positions as shown in Fig. 9 with multiplicity distributions for iTOF-module no.1 for two different beam positions, further away (P2) and closer (P3) to the SiPMs with mean multiplicities of $\overline{M}(P2) = 11.6$ and $\overline{M}(P3) = 11.4$. Thus a sufficient number of photons is generated and transported to the SIPMs, independent of the hit position, so that a high signal multiplicity is always achieved.

In general SiPMs allow precise time measurements with a resolution in the order of 100 ps but due to the variation of the transit time of the photons in the large scintillators the achievable time resolution is significantly worse. In Fig. 10 the distribution of time differences between iTOF-module no.3 and no.4 is shown for a centered stack position. A

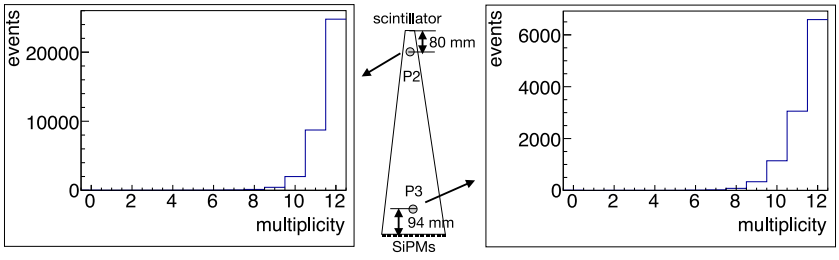

Fig. 9. Multiplicity distributions of iTOF-module no.1 for beam positions 80 mm below the short edge (left) and 94 mm above the long edge (right) as indicated in the center.

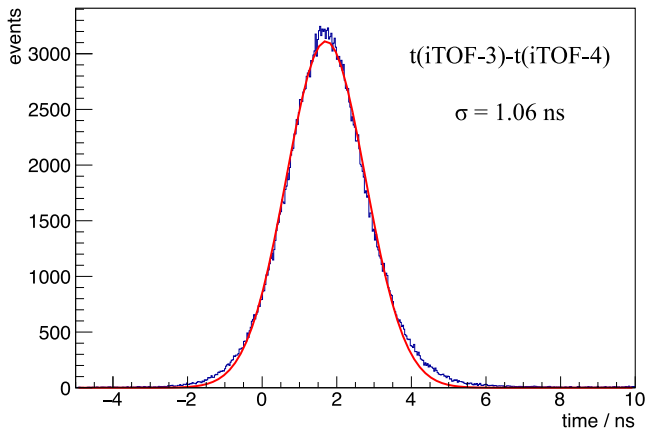

Fig. 10. Distribution of the time difference for the fast SiPM signals of iTOF-module no.3 and iTOF-module no.4. A width of $\sigma = 1.06$ ns is given from a gaussian fit which results in a single module time resolution of $\sigma \approx 750$ ps.

gaussian fit to the distribution gives a width of $\sigma = 1.06$ ns, which results in a time resolution of $\sigma \approx 750$ ps for a single iTOF-module, assuming the same resolution for both modules. The time difference between modules roughly compensates the variation of photon transit time because both modules were hit at the same position. But with the knowledge of the precise hit position which is available in the HADES experiment a further improvement of the time resolution is expected. For the application of the iTOF-detector as a trigger system, a time resolution of a few ns is sufficient.

For the test with cosmic particles the stack was rotated by 90°, so the normal to the module planes pointed vertically. Events were selected with clear coincident signals in the first and the last iTOF-module by requesting a multiplicity of 12 in both of these modules. Fig. 11 shows the signal multiplicity distributions for two modules in between. With cosmic particles all three scintillators in the modules (A, B, C) were irradiated as shown in Fig. 11. Also in this study multiplicities of 12 were achieved in more than 60% of the events on average for all scintillators of the modules 2 to 5. Compared to the proton beam data some events for M = 0 are visible which can be attributed to a not perfect geometrical overlap of the iTOF-modules in the stack. In case of the proton beam a well defined beam size with a diameter of about 1 cm ensured that each particle crossed all scintillators of the whole stack.

5. Conclusions and outlook

A new large area scintillator detector has been prepared for the HADES detector system to be used as a trigger system. Due to space limitations and location in a high magnetic field region silicon photomultipliers were used to detect the scintillation light resulting in a rather compact design. Each scintillator element was equipped with 12 SiPMs for the light collection. The trigger signal is generated based on the coincident detection of several SiPM signals. This allows a clear separation of signals induced by charged particles from the dark current in the SiPMs. The achieved detection efficiency for charged particles is practically 100% as determined from test measurements with proton beam and cosmic particles.

After the test measurements the iTOF-detector was installed at HADES and successfully taken into operation. In a beam time period of several weeks it was operated under very stable conditions without problems. Preliminary analyses of the detection efficiency are consistent with the test measurements. The detailed performance in the operation at HADES is presently under analysis.

Declaration of competing interest

The authors declare that they have no known competing financial interests or personal relationships that could have appeared to influence the work reported in this paper.

Data availability

Data will be made available on request.

Acknowledgment

This publication has partly received funding from the European Union's Horizon 2020 research and innovation programme under grant agreement STRONG – 2020 – No 824093.

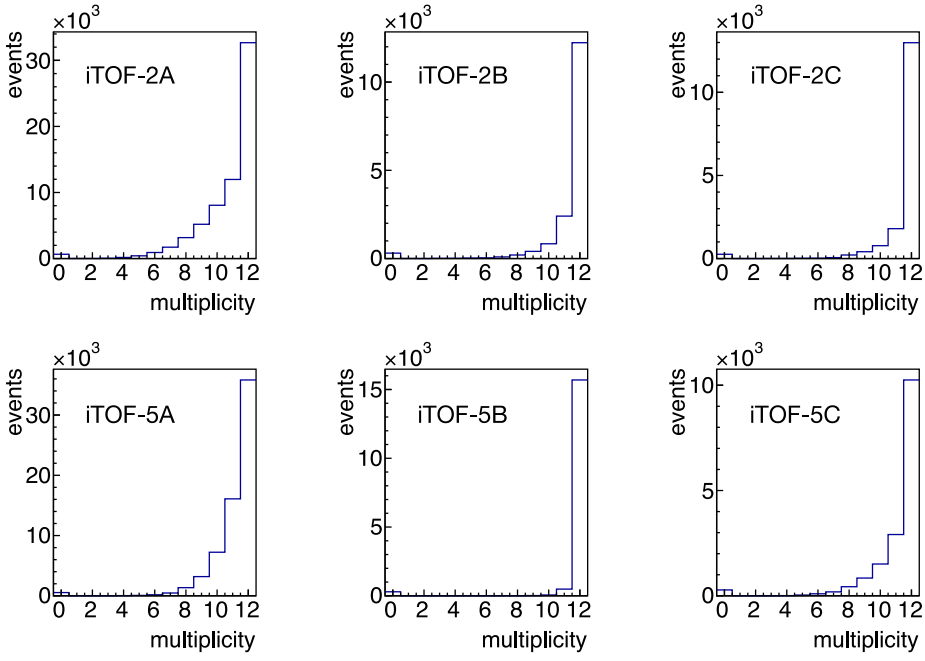

Fig. 11. Distribution of the fast SiPM signal multiplicity for the modules no.2 and no.5 resulting from a passage of cosmic particles. For a definition of a cosmic particle, events were selected with a multiplicity of 12 in the first and the last module of the stack. The event selection was performed separately for the three scintillators A, B and C.

References

[1] D. Renker, Geiger-mode avalanche photodiodes, history, properties and problems, Nucl. Instrum. Methods A 567 (2006) 48–56, http://dx.doi.org/10.1016/j.nima.2006.05.060.

[2] F. Simon, Silicon photomultipliers in particle and nuclear physics, Nucl. Instrum. Methods A 926 (2019) 85–100, http://dx.doi.org/10.1016/j.nima.2018.11.042.

[3] P. Moskal, et al., Positronium imaging with the novel multiphoton PET scanner, Sci. Adv. 7 (2021) eabh4394, http://dx.doi.org/10.1126/sciadv.abh4394.

[4] P. Moskal, et al., Testing CPT symmetry in ortho-positronium decays with positronium annihilation tomography, Nature Commun. 12 (2021) 5658, http://dx.doi.org/10.1038/s41467-021-25905-9.

[5] R. Schicker, et al., Acceptance and resolution simulation studies for the dielectron spectrometer HADES at GSI, Nucl. Instrum. Methods A 380 (1996) 586–596, http://dx.doi.org/10.1016/0168-9002(96)00732-2, arXiv:nucl-ex/9605004.

[6] HADES, 2022. https://www.gsi.de/forschungbeschleuniger/forschung_ein_ueberblick/hades_experiment.

[7] J. Adamczewski-Musch, et al., Production and electromagnetic decay of hyperons: A feasibility study with HADES as a phase-0 experiment at FAIR, Eur. Phys. J A57 (2010) 138, http://dx.doi.org/10.1140/epja/s10050-021-00388-w.

[8] Saint-Gobain, 2022, https://www.crystals.saint-gobain.com/radiation-detection-scintillators/plastic-scintillators.

[9] Onsemi, 2022, https://www.onsemi.com/products/sensors/photodetectors-sipm-spad.

[10] TRB, 2022, https://trb.gsi.de.

[11] A. Rost, et al., A flexible FPGA based QDC and TDC for the HADES and the CBM calorimeters, J. Instrum. 12 (2017) C02047, http://dx.doi.org/10.1088/1748-0221/12/02/C02047.

[12] A. Neiser, et al., TRB3: A 264 channel high precision TDC platform and its applications, J. Instrum. 8 (2013) C12043, http://dx.doi.org/10.1088/1748-0221/8/12/C12043.

[13] T. Tolba, D. Grzonka, T. Sefzick, J. Ritman, Irradiation studies of silicon photomultipliers with proton beam from the JULIC cyclotron, Nucl. Instrum. Methods A 1025 (2022) 166130, http://dx.doi.org/10.1016/j.nima.2021.166130.

[14] R. Maier, Cooler synchrotron COSY — Performance and perspectives, Nucl. Instrum. Methods Phys. Res. A 390 (1) (1997) 1–8, http://dx.doi.org/10.1016/S0168-9002(97)00324-0, URL https://www.sciencedirect.com/science/article/pii/S0168900297003240.